Structures of $NO_2^+(H_2O)_n$ and $(HNO_3)(H_3O^+)(H_2O)_{n-2}$ ($n = 2-4$) Clusters

R. C. Binning, Jr. and Yasuyuki Ishikawa*

Department of Chemistry, University of Puerto Rico, P.O. Box 23346, San Juan, PR 00931-3346

Received: March 23, 2000; In Final Form: June 29, 2000

The structures of more than thirty $H_{2n}NO_{n+2}^+$ ($n = 2-4$) complexes have been optimized in ab initio MP2/6-31+G* calculations. Relative energies of the species identified have been established in G2MP2 theoretical calculations and applied to an examination of the thermochemistry of the $NO_2^+(H_2O)_{n-1} + H_2O \rightarrow NO_2^+ + (H_2O)_n \rightarrow HNO_3(H_3O^+)(H_2O)_{n-2} \rightarrow HNO_3 + H_3O^+(H_2O)_{n-2}$ reactions. The nature of the most stable cluster varies with size. An ion-centered $NO_2^+(H_2O)_2$ is the global minimum energy structure on the $H_4NO_4^+$ surface, while an $HNO_3(H_3O^+)(H_2O)_2$ complex is most stable on $H_8NO_6^+$. On the $H_6NO_5^+$ surface $NO_2^+(H_2O)_3$, $HNO_3(H_3O^+)(H_2O)$ and $H_2NO_3^+(H_2O)_2$ clusters lie within 1 kcal/mol of each other.

1. Introduction

Interactions of nitronium ion with clusters of water molecules play a role in stratospheric chemistry.[1] It is believed that NO_2^+ arises on polar stratospheric cloud (PSC) particles as part of one pathway in the hydration of N_2O_5 to form HNO_3.[2] Once formed the hydrated ion reacts further with water, until a critical cluster size is reached, and nitric acid is formed

$$NO_2^+(H_2O)_{m-1} + H_2O \rightarrow HNO_3 + H_3O^+(H_2O)_{m-2} \quad (1)$$

Such processes contribute to the growth of the hydrated hydronium ion clusters that form the backdrop for much of stratospheric ion chemistry.[3] Nitric acid and its hydrates on PSCs in turn interact with the chlorine compounds primarily responsible for the polar ozone destruction cycle.[4] Despite their importance little is known in detail about the structures or relative stabilities of any but the simplest complexes of NO_2^+ and water.

$NO_2^+-H_2O$ has been studied experimentally and theoretically. In early flowing afterglow experiments Fehsenfeld et al.[5] determined that the species formed by direct complexation of NO_2^+ and water was identical to that formed by protonation of nitric acid. Subsequent ab initio calculations[6,7] confirmed the most stable form of $H_2NO_3^+$ to be the $NO_2^+(H_2O)$ complex, and found the geometry to be planar, C_{2v}. These calculations, and the mass-analyzed ion kinetic energy (MIKE) release experiments of Cacace et al.[8,9] also found an $ON(OH)_2^+$ structure about 10 kcal/mol higher in energy. Lee and Rice[6] performed accurate calculations on two isomers of this form of $H_2NO_3^+$. The dissociation energy of $NO_2^+(H_2O)$ has been determined experimentally[9,10] and theoretically[6,7] to lie in the range of 15−20 kcal/mol.

Grandinetti et al.[7] have performed Hartree−Fock (HF) and MP2/6-31G** calculations to explore the structures of isomers of $H_4NO_4^+$. Among the structures optimized was a D_{2h} $NO_2^+(H_2O)_2$ complex that they found to be the global minimum energy structure. They calculated the energy of $NO_2^+(H_2O) + H_2O \rightarrow NO_2^+(H_2O)_2$ to be 19.7 kcal/mol, some 2.8 kcal/mol less than the calculated hydration energy of NO_2^+.

Despite a relative dearth of structural and thermochemical information on $H_{2n}NO_{n+2}^+$ clusters for $n > 1$, they have, because of their importance in atmospheric chemistry, attracted experimental inquiry. Okumura and co-workers[11,12] and Stace and co-workers[13,14] have observed the fragmentation of nitronium − water clusters with as many as 10 water molecules mass spectrometrically. The studies agreed in finding a size threshold below which the major product of cluster fragmentation is a molecule of water, and at and above which the major product is a molecule of nitric acid. They disagreed as to whether the threshold is at three or at four molecules of water. Stace et al.[13] found decay to HNO_3 to occur in 70% of the fragmentations of $NO_2^+(H_2O)_3$ clusters, while Cao et al.[11,12] reported HNO_3 formation to be minor with these clusters, H_2O ejection occurring 85% of the time. They observed HNO_3 as the dominant product upon reaching the four−water clusters.

The principal differences in the experiments were that Okumura and co-workers[11,12] deployed an infrared (IR) laser pulse toward the end of the flight path of the clusters to photofragment them, whereas Angel and Stace[13,14] monitored the unimolecular fragmentation patterns by mass spectrometry alone. In the three−water clusters Cao et al.[11,12] did not observe the characteristic 3550 cm^{-1} NO−H stretch of HNO_3. They took that observation as evidence that HNO_3 was not present in the clusters, and that the formation of the small fraction of HNO_3 observed was being induced by the laser irradiation. They further noted wavelength dependence in the degree of HNO_3 loss, again indicating that IR excitation was promoting the formation.

Angel and Stace,[15] in a more recent MIKE experiment, have attempted to reconcile the differences in the results for the three−water clusters. They argued that it is possible for the majority of cluster ions at the critical size, $NO_2^+(H_2O)_3$, to be in the form of unreacted nitronium clusters, but that, when reaction does occur, the cluster binding energy for HNO_3 is small enough that the acid will be rapidly lost in unimolecular decay. Then, because the experiment of Angel and Stace[13,14] detected the products of clusters decaying over a fairly long time span ($\sim 10^{-5}$ s), it would detect the presence of HNO_3 resulting from fragmentation. Conversely, because Cao et al.[11,12] photfragmented clusters toward the end of the flight path, HNO_3 would already have departed and not be detected. This interpretation relies on reasonable assumptions about the relative

* Corresponding author. E-mail: ishikawa@rrpac.upr.clu.edu. Fax: (787) 751-0625.

10.1021/jp0010987 CCC: $19.00
Published on Web 08/08/2000

TABLE 1: Harmonic Vibrational Frequencies of the O−H Stretches and the NO_2 Asymmetric Stretch in $NO_2^+(H_2O)_n$ Complexes and of $NO^+(H_2O_2)(H_2O)_2$[a]

molecule		frequencies (cm^{-1})								
		H_2O								NO_2^+
NO_2^+										2496 (69)
H_2O		3800 (70)	3658 (12)							
$(H_2O)_2$		3788 (100)	3767 (137)	3655 (17)	3588 (277)					
$NO_2^+(H_2O)_2$	1A	3747 (289)	3747 (0)	3636 (23)	3635 (85)					2535 (91)
$NO_2^+(H_2O)_2$	1B	3746 (144)	3731 (190)	3629 (33)	3488 (444)					2510 (88)
$NO_2^+(H_2O)$	2A	3760 (141)	3751 (271)	3751 (0)	3643 (42)	3636 (9)	3636 (83)			2549 (87)
$NO_2^+(H_2O)_3$	2B	3760 (160)	3749 (140)	3720 (169)	3634 (40)	3630 (33)	3482 (426)			2523 (85)
$NO_2^+(H_2O)_3$	2C	3750 (302)	3750 (34)	3634 (40)	3633 (65)	3128 (1782)	3043 (1359)			2249 (164)
$NO_2^+(H_2O)$	3A	3766 (253)	3766 (0)	3755 (252)	3755 (0)	3645 (0)	3644 (65)	3636 (0)	3636 (72)	2559 (82)
$NO_2^+(H_2O)_4$	3B	3769 (244)	3769 (33)	3747 (249)	3746 (0)	3643 (9)	3643 (48)	3629 (42)	3629 (41)	2556 (80)
$NO_2^+(H_2O)_4$	3C	3753 (153)	3752 (145)	3737 (146)	3724 (169)	3638 (141)	3620 (37)	3604 (48)	3494 (284)	2542 (84)
$NO_2^+(H_2O)_4$	3D	3738 (312)	3738 (79)	3708 (194)	3708 (124)	3566 (141)	3565 (178)	3424 (711)	3405 (137)	2521 (73)
$NO_2^+(H_2O)_4$	3E	3774 (136)	3758 (181)	3752 (127)	3650 (18)	3633 (12)	3609 (64)	3580 (706)	3469 (460)	2520 (87)
$NO_2^+(H_2O)_4$	3F	3773 (138)	3762 (168)	3720 (153)	3715 (131)	3649 (30)	3624 (48)	3462 (451)	3379 (826)	2521 (85)
$NO_2^+(H_2O)_4$	3G	3752 (182)	3736 (141)	3708 (174)	3668 (253)	3619 (77)	3608 (50)	3517 (264)	3499 (329)	2508 (95)
$NO_2^+(H_2O)_4$	3H	3735 (195)	3732 (186)	3719 (174)	3711 (152)	3577 (104)	3540 (229)	3495 (341)	3355 (527)	2516 (77)
$NO_2^+(H_2O)_4$	3I	3750 (227)	3723 (185)	3722 (154)	3613 (19)	3600 (74)	3582 (162)	3278 (933)	2983 (1382)	2260 (161)
$NO_2^+(H_2O)_4$	3J	3734 (182)	3733 (87)	3676 (488)	3655 (0)	3622 (5)	3616 (188)	3567 (302)	3552 (38)	2504 (113)

molecule		frequencies (cm^{-1})							
		H_2O						H_2O_2	
$H_2O_2(H_2O)_3NO^+$	5D	3763 (151)	3737 (225)	3730 (137)	3642 (42)	3614 (36)	3566 (192)	3197 (1323)	2691 (2303

[a] Frequencies are scaled by 0.9760. Calculated IR intensities (atomic units) appear in parentheses. Each molecule that is depicted is accompanied by its figure designation.

stabilities among clusters. Clearly, detailed knowledge of the structures and energetics of the species likely to be present, and accurate thermochemical information about them, is indispensable to the ultimate evaluation of this and other interpretations of the fragmentation reactions.

Okumura and co-workers[11] did tentatively propose likely structures for the $NO_2^+(H_2O)_n$ ($n = 1-5$) clusters generated in their study. These structures were ion-centered, structures in which a central nitronium was symmetrically surrounded by molecules of water. They also estimated the thermochemistry of the $NO_2^+(H_2O)_{n-1} + H_2O \rightarrow NO_2^+(H_2O)_n \rightarrow H_3O^+(H_2O)_{n-1} + HNO_3$ reactions, extrapolating what is known about the one−water fragmentation to estimate the energetics of the reactions of the 2−4 water clusters. Fehsenfeld et al.,[16] on the other hand, pointed out that ion-centered structures are not the only structures to be considered, that hydrogen bonding among water molecules could promote the stability of other types of cluster.

We have begun a study of the structures and dynamics of nitronium ion−water clusters and have previously reported[17] on the dynamics of collisions between NO_2^+ and water tetramer. We report here the results of extensive computational exploration of the potential energy surfaces of $H_{2n}NO_{n+2}^+$ ($n = 2-4$), which must be understood before the reaction of nitronium with water to form HNO_3 can be properly understood. We have optimized the structures of a number of species germane to the subject of reaction of nitronium ion−water clusters to form nitric acid. In addition we have calculated their energies by the G2MP2 method, a method which has been shown to provide accurate thermochemical comparisons.

2. Methods

Cluster geometries were optimized in ab initio Hartree−Fock (HF) calculations with second-order Møller−Plesset (MP2) perturbative improvement. Calculations were done with Gaussian94.[18] 6-31+G* basis sets were employed in the geometry optimizations. The starting configurations for the geometry optimizations included arrangements that emphasized hydrogen bonded water structures with nitronium at the periphery, ion-centered arrangements, and combinations of these in the larger clusters.

At the MP2 minimum energy geometry of each species G2MP2 calculations were carried out. G2MP2[19,20] provides accurate energy differences by correcting an initial QCISD(T)/6-311G** energy for the effects of basis set truncation, zero-point energy and incomplete recovery of correlation energy. A higher level correction, E_{HLC}, is also added. $E_{HLC} = An_\beta - Bn_\alpha$, with $A = 4.81$ mhartree and $B = 0.19$ mhartree and n_α and n_β the number of α and β valence electrons, respectively, such that $n_\alpha \geq n_\beta$. Our G2MP2 procedure differs slightly from the standard form. MP2 optimizations are done with core orbitals frozen, while G2MP2 theory employs full MP2. Zero-point vibrational energies were calculated at the same level as the optimizations, and all basis sets employed diffuse functions, obviating the need for the G2MP2 correction for the addition of such functions. Thus, our G2MP2 calculations were based upon a QCISD(T)/6-311+G** calculation. G2MP2 energy differences may be expected to be accurate to within 2−3 kcal/mol. On a test set of 125 calculations of bond dissociation energies, proton affinities, electron affinities and ionization energies the maximum absolute deviation from experiment exhibited by the G2MP2 method was 6.3 kcal/mol, and the average deviation was 1.58 kcal/mol.[19]

3. Results and Discussion

Tables1 and 2 exhibit the calculated high-energy harmonic vibrational frequencies of most of the molecules of interest. The high-energy region is the realm of the O−H stretches often used to diagnose the compositions of clusters. The structures of the $H_{2n}NO_{n+2}^+$ clusters are displayed in Figures 1−5. Figures 6−8 diagram the energy differences among the species on the $n = 2-4$ potential surfaces. Table 1S contains the G2MP2 energies of each cluster optimized, and of some of their component species as well. We shall discuss the low-lying structures on the potential surfaces from small to large, and then comment

TABLE 2: Harmonic Vibrational Frequencies (in cm^{-1}) of HNO_3 and $H_2NO_3^+$ Scaled by 0.9760[a]

molecule		frequency								
		H_2O				H_3O^+			HNO_3^- $H_2NO_3^+$	
HNO_3									3542 (101)	
HOONO									3586 (55)	
H_2O		3800 (70)	3658 (12)							
H_3O^+						3527 (508)	3527 (508)	3416 (54)		
$H_5O_2^+$		3683 (376)	3683 (247)	3584 (12)	3576 (256)					
$H_7O_3^+$		3751 (308)	3750 (128)	3639 (9)	3637 (116)	3633 (268)	2697 (1115)	2580 (3627)		
$H_2NO_3^+$									3439 (442)	3412 (99)
$HNO_3(H_3O^+)$	1C					3615 (366)	3525 (208)	2201 (3154)	3465 (215)	
$HNO_3(H_3O^+)$	1D					3609 (370)	3519 (216)	2302 (3139)	3473 (210)	
$H_2NO_3^+(H_2O)$	1E	3763 (262)	3663 (81)						3189 (2235)	3022 (2)
$HNO_3(H_5O_2^+)$	2D	3741 (228)	3630 (63)			3616 (275)	3038 (1821)	2370 (3141)	3493 (171)	
$HNO_3(H_5O_2^+)$	2E	3743 (227)	3631 (65)			3614 (251)	2990 (1818)	2403 (3152)	3484 (174)	
$H_2NO_3^+(H_2O)_2$	2F	3733 (312)	3733 (120)	3620 (1)	3619 (174)				2176 (607)	2006 (5424)
$H_2NO_3^+(H_2O)_2$	2G	3737 (216)	3723 (218)	3623 (83)	3611 (92)				2106 (1663)	2002 (3838)
$H_2NO_3^+(H_2O)_2$	2H	3754 (184)	3650 (170)	3639 (74)	3076 (803)				2858 (3911)	2665 (13)
$HNO_3(H_7O_3^+)$	4A	3758 (213)	3756 (167)	3641 (44)	3640 (73)	3220 (1510)	2906 (1360)	2847 (2756)	3495 (153)	
$HNO_3(H_7O_3^+)$	4B	3760 (218)	3757 (166)	3643 (49)	3641 (70)	3253 (152)	2910 (1369)	2851 (2774)	3500 (152)	
$HNO_3(H_7O_3^+)$	4C	3749 (271)	3721 (319)	3634 (50)	3630 (224)	3572 (236)	2663 (1408)	2434 (3032)	3494 (200)	
$HNO_3(H_7O_3^+)$	4D	3764 (170)	3748 (212)	3643 (55)	3635 (61)	3612 (204)	2743 (1647)	2576 (4290)	2840 (1071)	
$HOONO(H_7O_3)^+$	5A	3766 (165)	3760 (195)	3645 (16)	3644 (75)	3630 (208)	2887 (1759)	2043 (3749)	3111 (1307)	
$HOONO(H_7O_3)^+$	5B	3717 (285)	3701 (265)	3549 (375)	3415 (786)	3634 (199)	2592 (1832)	2188 (2783)	3574 (87)	
$HOONO(H_7O_3)^+$	5C	3719 (266)	3710 (262)	3634 (211)	3470 (608)	3531 (589)	2525 (1882)	2338 (2735)	3571 (110)	

[a] The calculated IR intensities (in a.u.) appear in parentheses. Column subheadings indicate the principal origin of the motions associated with the frequencies, whether in H_2O or H_3O^+ O−H stretches, or the NO−H stretches of HNO_3 or $H_2NO_3^+$. Each molecule depicted in the figures is appropriately designated.

on the harmonic vibrational frequency shifts to be encountered among the clusters.

3.1. $H_4NO_4^+$. Grandinetti et al.[7] found the global minimum energy HF/6-31G** structure of $NO_2^+(H_2O)_2$ to be a planar D_{2h} complex, consisting of NO_2^+ flanked on either side by a water molecule, oxygens directed at nitrogen. We found this structure to be, not a minimum, but a saddle point at the MP2/6-31+G* level, which, when displaced, moved to the minimum energy structure depicted in Figure 1A. The potential surface thus changes significantly with the inclusion of electron correlation. To confirm the finding we reoptimized and recalculated the frequencies of the D_{2h} structure at the QCISD/6-311+G** level, again finding a saddle point. Another minimum energy structure, shown in Figure 1B, is essentially a complex between NO_2^+ and hydrogen bonded water dimer. The ion-centered global minimum energy complex (Figure 1A) lies 16.0 kcal/mol below $NO_2^+(H_2O) + H_2O$; the nitronium−water dimer complex lies 11.8 kcal/mol below. Two minimum energy structures of $HNO_3-H_3O^+$ (Figure 1C,D) were found. The two structures are similar, but in the lower-energy of the two the hydronium ion is coordinated to the two (more negative) naked oxygens of HNO_3, whereas in the higher-energy form the second nearest neighbor is the OH oxygen atom of HNO_3. Energetically the complexes are nearly degenerate, separated by 0.7 kcal/mol. The more stable of the two is 25.3 kcal/mol beneath $HNO_3 + H_3O^+$ and 7.8 kcal/mol above the more stable of the $NO_2^+(H_2O)_2$ complexes.

Grandinetti et al. found an $H_2NO_3^+(H_2O)$ complex at the HF/6-31G** level, with the water molecule oriented perpendicular to the plane of the most stable conformer of $H_2NO_3^+$. In early HF/4-31G optimizations Nguyen and Hegarty[21] identified three such conformers. The $H_2NO_3^+$ conformers are not depicted, but their energies appear in Table 1S. Our attempts to locate the $H_2NO_3^+(H_2O)$ structure of Grandinetti et al. at the MP2/6-31+G* level resulted only in one of the $HNO_3-H_3O^+$ complexes illustrated in Figure 1. We did optimize one high-energy $H_2NO_3^+(H_2O)$ complex (Figure 1E) in which the O of the water appears to be held in chelae formed by the hydrogens of the trans-trans $H_2NO_3^+$ conformer noted by Nguyen and Hegarty.[21] Its energy is listed in Table 1S. However, the fact that optimizations attempted from several different starting configurations of $H_2NO_3^+ + H_2O$ led to $HNO_3(H_3O^+)$ indicates that no-barrier paths exist between the two types of species.

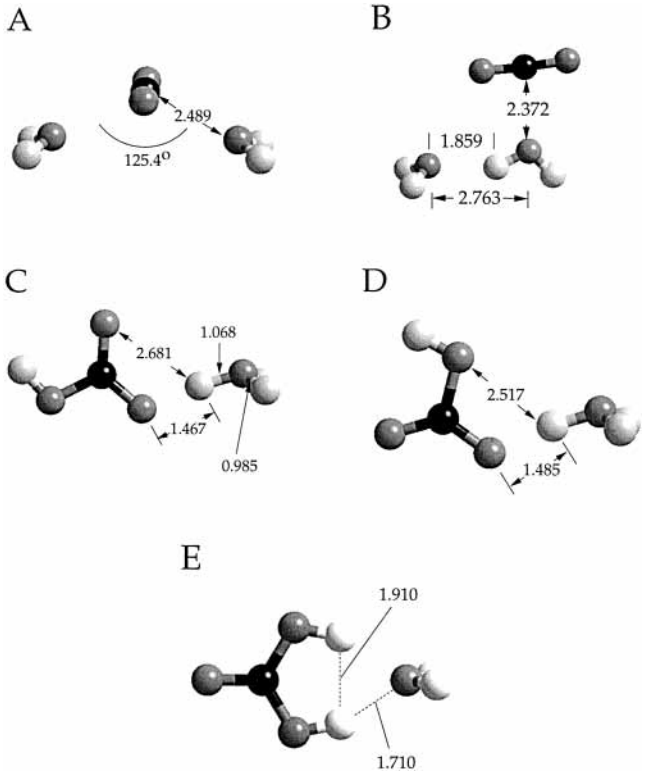

Figure 1. MP2/6-31+G* equilibrium geometries of $H_4NO_4^+$ clusters. Distances shown are in Å.

3.2. $H_6NO_5^+$. The G2MP2 potential energy surface is fairly complex, with five nearly energetically degenerate species (see Figure 7), three of them structurally distinct. The global minimum is an $HNO_3(H_3O^+)(H_2O)$ complex (Figure 2D), and

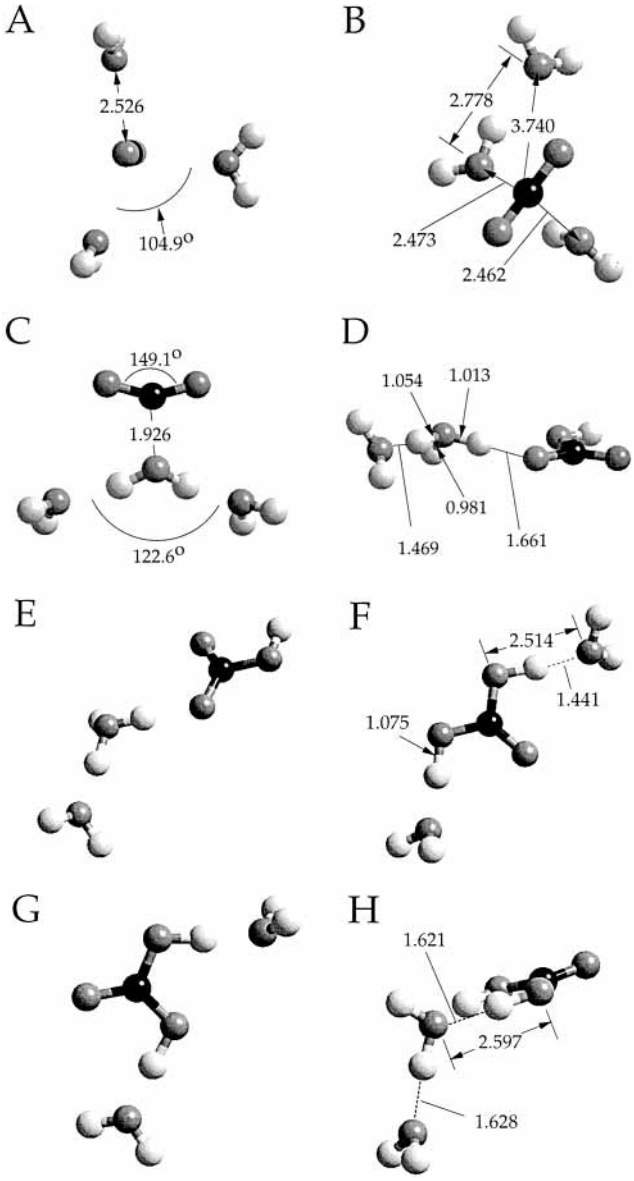

Figure 2. MP2/6-31+G* equilibrium $H_6NO_5^+$ structures. Distances are in Å.

it lies only 0.60 kcal below a similar complex (Figure 2E). These are centered about hydronium ion, and differ in the attitude of coordination of nitric acid to the ion. Lying only 0.33 kcal/mol above the global minimum is an $H_2NO_3^+(H_2O)_2$ complex (Figure 2F). This consists of the lower-energy of the two $H_2NO_3^+$ structures identified by Lee and Rice,[6] one molecule of water coordinated to each hydrogen. A second such complex (Figure 2G), of two waters attached to the second of the complexes noted by Lee and Rice, is only slightly higher in energy. The third (Figure 2H) is 11.5 kcal/mol above the global minimum. The lowest energy two−water complex was optimized from an $HNO_3(H_3O^+)(H_2O)$ initial structure, indicating that no-barrier paths exist between the two types of cluster, just as is true for the species on the $H_4NO_4^+$ surface.

The three $NO_2^+(H_2O)_3$ complexes are higher in energy than the two nitric acid and two of the protonated nitric acid complexes, but the most stable (Figure 2A) lies less than 1 kcal/mol above the global minimum. This is an ion-centered, distorted D_{3h}, complex. The optimum D_{3h} structure is a saddle point on the surface. Lying 4.2 kcal/mol above the complex of Figure 2A is a structure that appears to be a loose interaction between NO_2^+ and a distorted cyclic water trimer (Figure 2B).

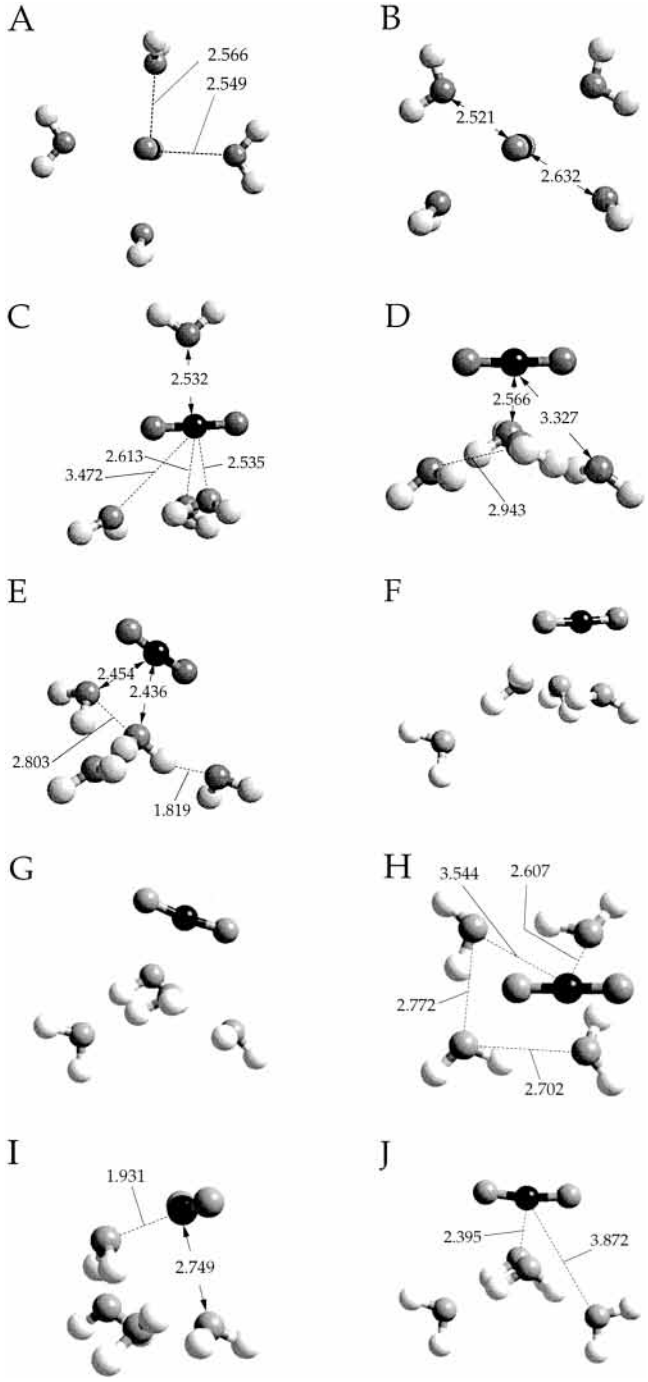

Figure 3. Equilibrium $NO_2^+(H_2O)_4$ complexes, structures on the $H_8NO_6^+$ energy surface. Distances are in Å.

The structures of the water trimers have been examined by Mó et al.[22] In the third of the $NO_2^+(H_2O)_3$ complexes (Figure 2C) NO_2^+ is attached to the central oxygen of a double hydrogen bond donor water trimer. The energy of the double-donor structure, labeled DD, is presented in Table 1S, but not depicted. The attachment of nitronium appears to be strong; the N−water-O bond length is short (1.926 Å), NO_2^+ is bent (O−N−O = 149.1°) and the MP2/6-31+G* optimum N−O bond lengths are longer than they are in free NO_2+ (1.176 versus 1.157 Å). This complex lies 8.68 kcal/mol above the global minimum at the G2MP2 level.

3.3. $H_8NO_6^+$. The surface exhibits great variety. We have identified ten $NO_2^+(H_2O)_4$ complexes (Figure 3), four $HNO_3(H_3O^+)(H_2O)_2$ nitric acid complexes (Figure 4), three $HOONO(H_3O^+)(H_2O)_2$ peroxynitrous acid complexes and one NO^+-

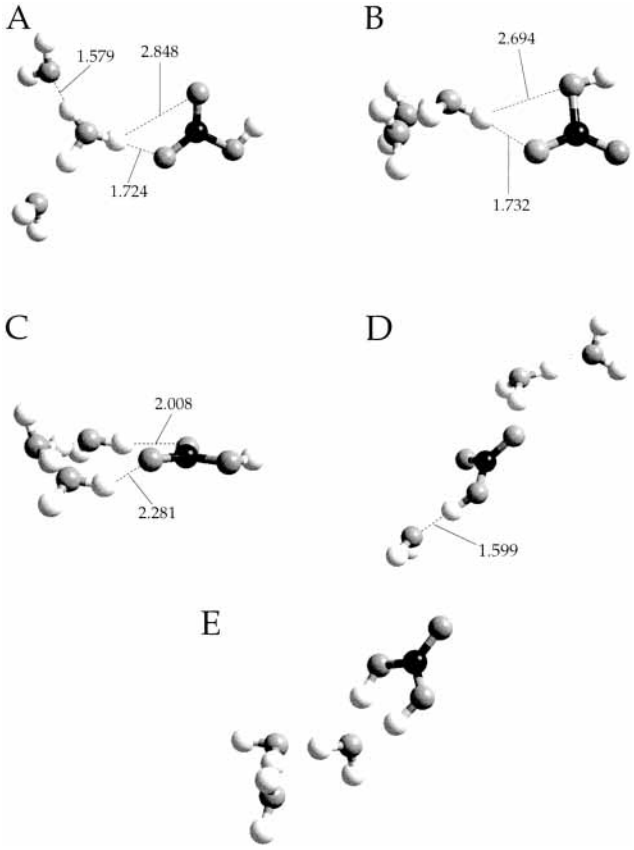

Figure 4. Stable minimum energy $HNO_3(H_3O^+)(H_2O)_2$ structures and one $H_2NO_3^+(H_2O)_3$ structure on the $H_8NO_6^+$ surface.

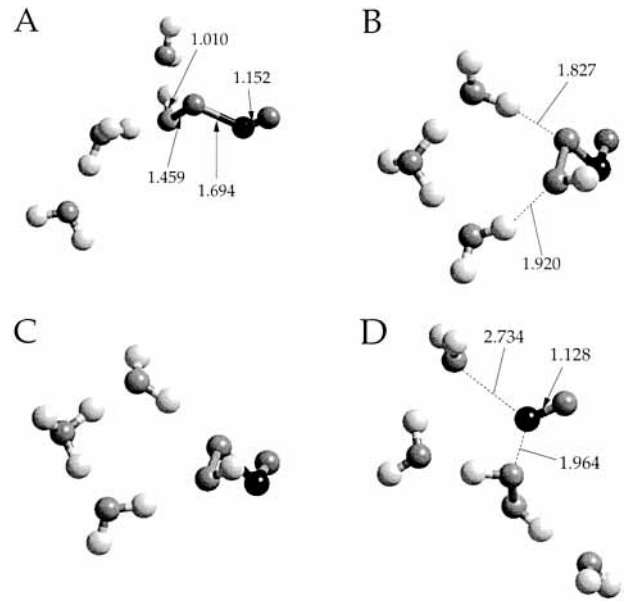

Figure 5. Equilibrium MP2/6-31+G* higher energy, $HNO_3(H_3O^+)(H_2O)_2$ and $NO^+(H_2O_2)(H_2O)_3$, complexes on the $H_8NO_6^+$ energy surface,.

$(H_2O_2)(H_2O)_3$ (Figure 5) within a 40 kcal/mol range of energies. Only one stable $H_2NO_3^+(H_2O)_3$ species (Figure 4E), however, was identified. It consists of the complex of Figure 2H with an additional water attached to the trailing water of that species. With the three−water, as with the one- and two−water complexes of $H_2NO_3^+$, no-barrier paths exist to HNO_3 complexes. The low-energy complexes are the nitric acid complexes, all of which lie lower in energy than the nitronium ion−water complexes. All of those, in turn, lie energetically beneath the peroxynitrous acid and hydrogen peroxide complexes. The hydrogen peroxide-nitrosonium cluster is highest in energy.

The trends in energy noted in the smaller complexes continue with these. The most stable of the $NO_2^+(H_2O)_4$ complexes are the ion-centered species. Thus, the assumption by Cao et al.[11] that the most stable nitronium−water complexes possessed ion-centered structures is supported by the calculations for the two-, three- and four−water complexes. We found two ion-centered structures, with distorted D_{4h} geometries, the oxygens of the water molecules oriented toward nitrogen, and linear NO_2^+ perpendicular to the plane of the oxygens (Figure 3A,B). Four of the $NO_2^+(H_2O)_4$ complexes (Figure 3D,G,H,J) have nitronium ion coordinated to cyclic water tetramers. In the lowest energy of these (Figure 3D) NO_2^+ lies diagonally across a structure reminiscent of the lowest-energy of the water tetramers, a square with each oxygen both hydrogen bond donor and acceptor. Adding NO_2^+ buckles the square, but the hydrogen bond structure remains intact. In the complex of Figure 3H the approximate planarity of the water tetramer structure is maintained. The structures of the water tetramers are not shown, but the energies of the four known minimum energy structures are displayed in Table 1S, with the labels assigned by Kim et al.[23] In the nitronium−water tetramer complexes only the cyclic tetramer structures could be said to have retained their identities.

The remainder of the $NO_2^+(H_2O)_4$ complexes (Figure 3C,E,F,I) may be viewed as structures in which NO_2^+ is attached to water trimer structures, with an additional water at the perimeter. In the lowest energy of these (Figure 3C) the $NO_2^+(H_2O)_3$ structure of Figure 2B is evident, and the fourth water is independently coordinated to NO_2^+. This complex may also be viewed as a distortion of a tetrahedron of waters coordinated to a central NO_2^+. In the very similar structures of Figure 3E,F the additional water molecule is attached by hydrogen bond to one of the waters of the cyclic trimer. Finally, in the structure of Figure 3I we see the structure of Figure 2C, with nitronium strongly attached to the central water molecule in a double-donor trimer, the fourth water molecule coordinated both to NO_2^+ and to one of the molecules of the trimer.

The four nitric acid complexes (Figure 4), although structurally diverse, all lie within 2 kcal/mol of each other at the G2MP2 level, energetically degenerate to within the precision of the method. The two low-energy complexes are ion-centered. The global minimum energy $HNO_3(H_3O^+)(H_2O)_2$ structure (Figure 4A) is one in which HNO_3 coordinates to hydronium ion at the two most negative atoms, the naked oxygens. In the other (Figure 4B) secondary coordination to the hydrogen-bearing oxygen is seen. A third complex is a cyclic structure (Figure 4C) in which HNO_3 is coordinated to two waters which in turn are attached to hydronium. Highest in energy is a water−nitric acid-hydronium ion−water chain structure (Figure 4D), the only structure in which HNO_3 is a hydrogen bond donor.

Several peroxynitrous acid−water complexes were optimized during searches for $NO_2^+(H_2O)_4$ structures that began from high-energy starting geometries. HOONO has been detected in the stratosphere, and it is known to be a product of radical recombination of hydroxyl and nitrogen dioxide.[24] There is little direct evidence of its generation in ion−molecule reactions on PSCs, but energetically $HOONO(H_3O^+)(H_2O)_2$ lies beneath separated NO_2^+ and four waters. In addition it has been proposed as an intermediate in processes in aqueous solution.[25] McGrath and Rowland[26] have examined isolated HOONO computationally. They found three conformer minima, and calculated their relative energies in G2 and G2MP2 calculations. They were found to lie within 3.1 kcal/mol of each other in energy. The

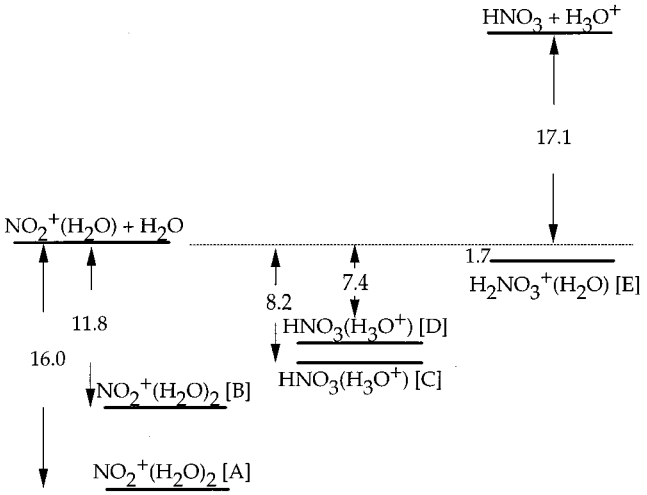

Figure 6. Energy diagram (kcal/mol) of $H_4NO_4^+$ complexes relative to $NO_2^+(H_2O) + H_2O$. Structures are depicted in Figure 2, and their letter designations within that figure appear adjacent to some of the complexes.

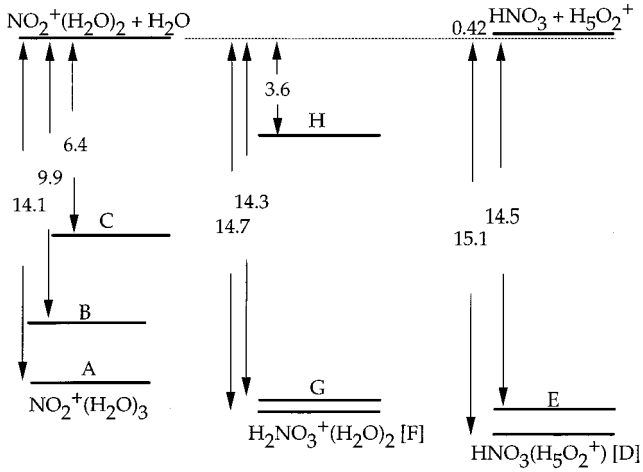

Figure 7. Diagram of energies (in kcal/mol) of $H_6NO_5^+$ complexes relative to the low-energy form of $NO_2^+(H_2O)_2$ (Figure 2A) + H_2O. Structures are depicted in Figure 3, and their letter designations within that figure label the energy levels.

hydrated complexes optimized in this study all involve the trans-perp conformer of McGrath and Rowland. The question of whether other conformers exist in hydration clusters lies somewhat beyond the scope of this study.

We identified three hydrated peroxynitrous acid complexes (Figure 5A−C). Two of these (Figure 5B,C) are similar cyclic structures with hydronium coordinated to two waters, each hydrogen-bonded to peroxynitrous acid. In one (Figure 5B) the free hydrogen of hydronium is trans to the acid hydrogen while the free hydrogens of the waters are cis, whereas in the other (Figure 5C) the hydronium hydrogen is cis and the water hydrogens trans. The third structure (Figure 5A) is a linear water-hydronium-HOONO−water structure. The structures are essentially degenerate energetically; they lie within 0.3 kcal/mol of each other at the G2MP2 level. These types of structures were found with nitric acid, and if the analogy holds, there should also be stable ion-centered configurations of peroxynitrous acid and water.

The $NO^+(H_2O_2)(H_2O)_3$ complex (Figure 5D), highest in energy among the complexes, is a linear water−water-(H_2O_2−NO^+)−water structure. Mulliken population analysis places a +0.74 charge on NO^+, the remainder residing on the peroxide.

3.4. Thermochemistry of Fragmentation. Okumura and co-workers[11] have estimated cluster dissociation enthalpies for $NO_2^+(H_2O)_n \rightarrow NO_2^+(H_2O)_{n-1} + H_2O$ for $n = 2-4$, extrapolating from the experimental $T = 0$K value of 14.8 ± 2.3 kcal/mol determined by Sunderlin and Squires[10] for $NO_2^+(H_2O)$. They estimated enthalpies of 12.5, 10, and 8.5 kcal/mol, respectively, for dissociation of the two, three and four water clusters. Because this sequence led them to estimates of the binding energies of HNO_3 to $H_3O^+(H_2O)$ and to $H_3O^+(H_2O)_2$ that were somewhat too low, they inferred that the sequence of nitronium−water binding energies was too low. Basing their estimations on the result of Cacace et al.[9] of 19.6 ± 2 kcal/mol for the one−water cluster, each estimate would increase by 4.8 kcal/mol. The G2MP2 energies (see Table 1S, Figures 6−8) for the loss of one molecule of water from each of the $n = 1-4$ water nitronium complexes are, respectively, 18.1, 16.0, 14.1, and 11.7 kcal/mol. The calculated cluster dissociation energies support the conjecture of Okumura and co-workers that the numbers in the sequence derived from the experimental dissociation energy of Sunderlin and Squires[10] are too low.

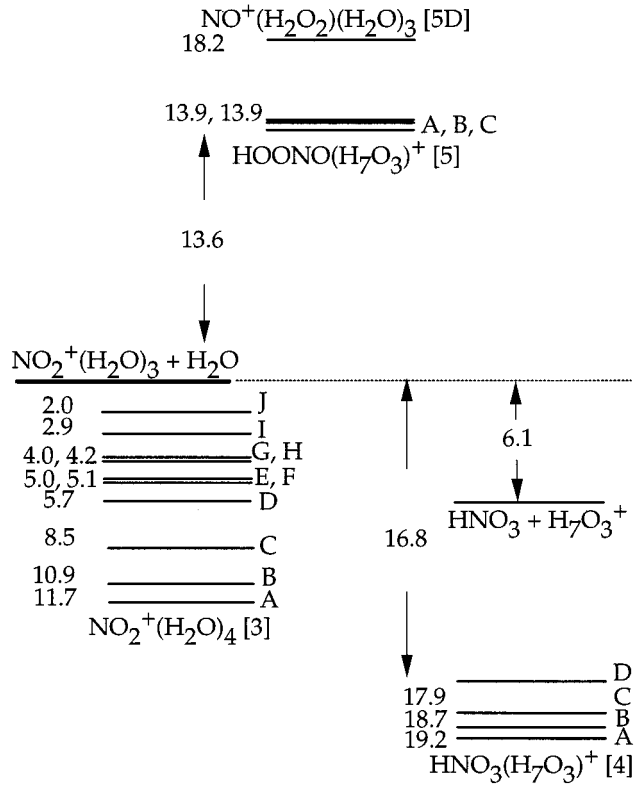

Figure 8. Diagram of energies (in kcal/mol) of $H_8NO_6^+$ complexes relative to the low-energy form of $NO_2^+(H_2O)_3$ (Figure 3A) + H_2O. Structures are depicted in Figures 4−6. The figure number accompanies the formula of each type of complex, and letter designations within that figure label the energy levels.

Figures 6−8 limn the thermochemistry of the

$$NO_2^+(H_2O)_{n-1} + H_2O \rightarrow NO_2^+(H_2O)_n \rightarrow HNO_3(H_3O^+)(H_2O)_{n-2} \rightarrow H_3O^+(H_2O)_{n-2} + HNO_3 \quad (2)$$

reaction sequence. As the number of water molecules increases the number available to stabilize the hydronium ion increases, and the process as a whole becomes more exothermic. Whereas at $n = 2$ the process $NO_2^+(H_2O) + H_2O \rightarrow H_3O^+ + HNO_3$ is endothermic, with a reaction energy of +17.1 kcal/mol, the $n = 3$ reaction is thermoneutral, with a reaction energy of −0.4

kcal/mol. By $n = 4$ the process is exothermic, with a G2MP2 energy change of −6.1 kcal/mol. On the basis of their observations Cao et al.[11] estimated that the $n = 3$ reaction, $NO_2^+(H_2O)_2 + H_2O \rightarrow H_5O_2^+ + HNO_3$, was approximately thermoneutral. On the basis of the absence of observed conversion of $NO_2^+(H_2O)_3$ to $HNO_3(H_5O_2^+)$, they postulated that the nitronium complex must be lower in energy than the acid. G2MP2 energetically the two complexes are almost the same energy, but this is still consistent with the experimental observation.

Angel and Stace[15] suggested that the majority of the $NO_2^+(H_2O)_3$ clusters produced might remain unreacted, while those that do react rapidly expel HNO_3. That would explain why one group[13,14] observed fragmentation of $NO_2^+(H_2O)_3$ while the other[11,12] did not. It might be the case that most of the three−water clusters remain unreacted if $NO_2^+(H_2O)_3$ were more stable than $HNO_3(H_5O_2^+)$. Again the G2MP2 results assign nearly equal energies to the most stable forms of the two clusters, and there are two isomers of $NO_2^+(H_2O)_3$ of higher energy. Furthermore, $HNO_3(H_5O_2^+)$ is about 15 kcal/mol below $HNO_3 + H_5O_2^+$ in energy. Fragmentation to HNO_3 is therefore definitely endothermic. It may still be a dominant process in the experiments discussed here. The ion clusters, generated by electron impact[13,14] or by glow discharge,[11,12] are likely to be internally energetic, and the processes that lead to the experimental observations probably take place considerably above the minimum energy surface. In addition both groups found fragmentation to HNO_3 to be the dominant process in the four−water clusters although $HNO_3(H_7O_3^+)$ is more than 10 kcal/mol beneath $HNO_3 + H_7O_3^+$.

Angel and Stace[15] observed that $NO_2^+(H_2O)_{n-1} + H_2O \rightarrow H_3O^+(H_2O)_{n-2} + HNO_3$ is not promoted by collisional activation, but that, having taken place, unimolecular decay favors the loss of acid. Indeed $HNO_3 + H_5O_2^+$ lies 8.2 kcal/mol below $HNO_3(H_3O^+) + H_2O$, and $HNO_3 + H_7O_3^+$ 5.2 kcal/mol below $HNO_3(H_5O_2^+) + H_2O$ in energy. A previous ab initio direct molecular dynamics simulation[17] of collisions between NO_2^+ and $(H_2O)_4$ provides some insight into the observation that the reaction to form nitric acid is not promoted by collisional activation. That study noted that the success of the reaction was governed by a series of correlated motions, and that when the reactants are properly positioned, the energetic barrier is low. On the other hand the expulsion of HNO_3 from a cluster in which it already exists would depend strongly upon internal cluster energy.

The energy differences among the product processes in successive figures from Figures 6 to 8 are the successive hydration energies of hydronium ion−water clusters. These have been measured.[27] The experimental $\Delta H_{0,1} = -31.6$ kcal/mol, whereas the G2MP2 energy change for $H_3O^+ + H_2O \rightarrow H_5O_2^+$ is −33.5. $\Delta H_{1,2} = -19.5$ kcal/mol, while the G2MP2 hydration energy is −19.8 kcal/mol.

3.5. IR Frequency Shifts. Infrared spectroscopy is one of the primary means of characterizing clusters. The cluster fragmentation experiments of Cao et al.[11,12] relied on IR spectra in the region of absorption by the O−H stretches to monitor cluster composition. The characteristic NO−H stretch of HNO_3 at around 3550 cm^{-1} was used to signal the presence of HNO_3 in the clusters. Vibrational frequencies can exhibit sizable shifts upon solvation. Our calculations offer a broad internally consistent survey of frequency shifts in the nitronium and nitric acid clusters. Tables 1 and 2 list the high energy harmonic vibrational frequencies derived from the MP2/6-31+G* calculations. Besides the O−H stretches the asymmetric stretching frequency of NO_2^+ has been included because its energy (>2500 cm^{-1}) places it in the realm of the O−H stretches. The frequencies in the tables are classified according to the nature of the normal mode giving rise to each frequency; water or NO_2^+ stretches in Table 1, and water, hydronium and nitric or protonated nitric acid O−H stretches in Table 2. Table 1 also displays the harmonic frequencies calculated for $NO^+(H_2O_2)(H_2O)_3$. For this complex the first six columns show the frequencies of water stretches, and the rightmost two columns the frequencies for hydrogen peroxide. The NO^+ stretch occurs at a lower frequency. The frequencies in the tables have been scaled (by 0.9760) to minimize the average deviation from the experimental gas-phase vibrational frequencies of HNO_3 and H_2O[12] and of $H_5O_2^+$ and $H_7O_3^+$.[28] Scaling harmonic frequencies to experimental fundamentals corrects in an average way for the effects of anharmonicity.

The scaled calculated harmonic frequencies represent the experimental spectra fairly well. The experimental spectrum of H_2O monomer shows the symmetric stretch occurring at 3657 cm^{-1} and the asymmetric at 3756 cm^{-1}.[12] The calculated frequencies (Table 1), respectively, are 3658 and 3800 cm^{-1}, slightly underestimating the spacing of the bands. The calculated nitric acid NO−H frequency (Table 2), 3542 cm^{-1}, is near the experimental 3551 cm^{-1}.[12] The calculated frequencies of water dimer are included in Table 1 to indicate the effect of hydrogen bonding. The frequencies, 3788 and 3655 cm^{-1}, of the water molecule that is the hydrogen bond acceptor are little perturbed. The symmetric stretch of the hydrogen bond donor shows a red shift with an enhancement in intensity, and the asymmetric stretch displays both to a greater extent.

$H_5O_2^+$ is not depicted, but its geometry and IR spectrum have been examined by Termath and Sauer[29] in density functional theoretical calculations and by Valeev and Schaefer[30] in very accurate coupled cluster calculations. It consists of two waters bound by a bridging hydrogen in a C_2 configuration.[30] The experimental spectrum[28] has bands at 3609 and 3684 cm^{-1}, the latter showing extensive rotational structure. The calculated frequencies appear at 3576 cm^{-1}, 3584, 3683, and 3683 cm^{-1}. Both spectra are consistent with a structure consisting of two weakly interacting water units. The difference between calculated asymmetric and symmetric stretching frequencies is about 30 cm^{-1} too high. The spread is reduced somewhat but persists in the accurate calculations of Valeev and Schaefer[30] and is thus likely related to the use of the harmonic approximation. Although the two symmetric stretches are split, they are consistent with the single experimental band, which is broader than the calculated splitting. In addition the experimental band at the higher frequency is more intense, consistent with the calculated intensities.

$H_7O_3^+$ has also been examined by Termath and Sauer.[29] It consists of a central H_3O^+ hydrogen bonded to two water molecules. The calculated spectrum gives the frequencies for the water vibrations at 3637, 3639, 3750, and 3751 cm^{-1}. The hydronium ion frequencies show the red shifts arising from hydrogen bonding. While the calculated spectrum of the hydronium ion displays a symmetric stretch at 3416 cm^{-1} and a degenerate asymmetric stretch at 3527 cm^{-1}, the corresponding lines in $H_7O_3^+$ lie at 2580, 2697, and 3633 cm^{-1}. The two low-frequency lines belong to the hydrogens participating in the hydrogen bonds, and they display enhanced intensity compared to the isolated ion. The experimental spectrum[28] displays high-frequency bands at 3637, 3667, and 3722 cm^{-1}. The authors assigned these to the water asymmetric stretch, the H_3O^+

unoccupied hydrogen, and the water symmetric stretch, respectively, consistent with the spectrum shown in Table 2.

HNO_3 in the hydronium ion−water clusters is peripheral, coordinated to the ion. The NO−H stretch shifts to lower frequency in the clusters, but the shifts are not large. In HNO_3-(H_3O^+) the average of the shifts in the two isomers is 73 cm^{-1}, in $HNO_3(H_5O_2^+)$ the average red shift is 54 cm^{-1}, and in the three $HNO_3(H_7O_3^+)$ clusters in which HNO_3 coordinates at the bare oxygens, the shift is 46 cm^{-1}. In the cluster (Figure 4D) in which NO−H participates in a hydrogen bond, however, the downshift is 700 cm^{-1}. The effect is similar to peroxynitrous acid. The calculated monomer stretching frequency is 3586 cm^{-1}. The experimental frequency in solid argon lies at 3546 cm^{-1}.[24] In the two $HOONO(H_7O_3^+)$ clusters in which NO−H is not involved in a hydrogen bond, an average frequency shift of 14 cm^{-1} is noted (Table 2), whereas in the cluster (Figure 5A) in which there is participation in hydrogen bonding the frequency shifts downward 475 cm^{-1}.

The $H_2NO_3^+$ monomer isomers shows a pair of closely spaced lines at around 3400 cm^{-1}. Lee and Rice[6] found the scaled frequency to be about 3450 cm^{-1} in the two isomers they found. In the $H_2NO_3^+(H_2O)$ cluster we optimized (Figure 1E) both hydrogens are coordinated to the water, the frequencies separate, and there are substantial shifts of 250 and 390 cm^{-1}. There are three $H_2NO_3^+(H_2O)_2$ clusters. One (Figure 2H) consists of the cluster of Figure 1E with an additional water molecule hydrogen bonded to the one in the cluster. In this cluster the NO−H frequencies show additional downshifts, of 581 cm^{-1} and of 747 cm^{-1} from the monomer frequencies, and further separation. In the other two $H_2NO_3^+(H_2O)_2$ complexes each NO−H is hydrogen bonded to a separate water molecule, and the shifts are more pronounced, ranging from 1206 to 1368 cm^{-1}. The shifts due to hydrogen bonding are potentially valuable in detecting the presence of $H_2NO_3^+(H_2O)$. While the presence of H_3O^+ would be likely to obscure the NO−H bands of H_2-NO_3^+, the shifts accompanying the addition of a water should make their presence unambiguous. The same is potentially true for $H_2NO_3^+(H_2O)_2$, although in two of the isomers the shifts are great enough to bring the NO−H stretching frequencies into the more crowded 2000−2200 cm^{-1} region of the spectrum.

The effect of clustering on the NO_2^+ asymmetric stretch is not pronounced (see Table 1). There is a small blue shift in each instance with the exception of the two clusters in which nitronium is strongly enough attached to a water molecule to display significant geometry changes from the isolated ion. One is a three−water cluster (Figure 2C) and the other a four−water cluster (Figure 3I). In these the frequency red shifts by more than 200 cm^{-1}, indicating a weakening of the N−O bonds. The O−H frequencies of the water to which nitronium is attached show similar trends. Rather than the downward shifts of 50−300 cm^{-1} typical of hydrogen bonded waters, the O−H stretches of the double-donor water molecules in these complexes display shifts of from 500 to 700 cm^{-1} compared to isolated water.

3.6. Summary. MP2/6-31+G* optimizations have located a variety of species on the $H_{2n}NO_{n+2}^+$ ($n = 2-4$) potential energy surfaces, and G2MP2 calculations have provided energy data crucial to understanding the processes that occur on these surfaces. These data largely confirm the conclusions drawn by the experimentalists who have examined the systems. The most stable forms of the nitronium− and nitric acid−water clusters have been confirmed to be ion-centered complexes, and the thermochemistry of the reactions of NO_2^+−water clusters to form nitric acid has been established. In the process a variety of higher-energy complexes involving, not only NO_2^+ and HNO_3, but also $H_2NO_3^+$, NO^+ and HOONO have been identified. The question of the critical cluster size needed to form HNO_3 has not been definitively answered. It appears not to be susceptible to resolution solely on energetic arguments; rather the answer resides in the dynamic aspects of the cluster reactions.

Acknowledgment. The authors are grateful to Professor M. Okumura for discussions that proved helpful in conducting this research, to NASA for funding through the EPSCoR program, and to the RCMI Center for Molecular Modeling and Computational Chemistry for providing computing facilities.

Supporting Information Available: Table 1S, a table of the G2MP2 and G2MP2-component energies of all species discussed is available free of charge via the Internet at http://pubs.acs.org.

References and Notes

(1) Böhringer, H.; Fahey, D. W.; Fehsenfeld, F. C.; Ferguson, E. E. *Planet. Space Sci.* **1983**, *31*, 185.
(2) McCoustra, M. R. S.; Horn, A. B. *Chem. Soc. Rev.* **1994**, *23*, 195.
(3) Arijs, E. *Planet. Space Sci.* **1992**, *40*, 255.
(4) Molina, M. J.; Zhang, R.; Wooldridge, P. J.; McMahon, J. R.; Kim, J. E.; Chang, H. Y.; Beyer, K. D. *Science* **1993**, *261*, 1418.
(5) Fehsenfeld, F. C.; Howard, C. J.; Schmeltekopf, A. L. *J. Chem. Phys.* **1975**, *63*, 2835.
(6) Lee, T. J.; Rice, J. E. *J. Phys. Chem.* **1992**, *96*, 650; *J. Am. Chem. Soc.* **1992**, *114*, 8247.
(7) Grandinetti, F.; Bencivenni, L.; Ramondo, F. *J. Phys. Chem.* **1992**, *96*, 4354.
(8) Cacace, F.; Attina, M.; de Petris, G.; Speranza, M. *J. Am. Chem. Soc.* **1989**,*111*, 5481; **1990**, *112*, 1014.
(9) Cacace, F.; Attina, M.; de Petris, G.; Speranza, M. *J. Am. Chem. Soc.* **1994**, *116*, 6413.
(10) Sunderlin, L. S.; Squires, R. R. *Chem. Phys. Lett.* **1993**, *222*, 333.
(11) Cao, Y.; Choi, J.-H.; Haas, B.-M.; Okumura, M. *J. Phys. Chem.* **1994**, *98*, 12176.
(12) Cao, Y.; Choi, J.-H.; Haas, B.-M.; Johnson, M. S.; Okumura, M. *J. Chem. Phys.* **1993**, *99*, 9307.
(13) Stace, A. J.; Winkel, J. F.; Atrill, S. R. *J. Chem. Soc., Faraday Trans.* **1994**, *90*, 3469.
(14) Angel, L.; Stace, A. J. *J. Chem. Soc., Faraday Trans.* **1997**, *93*, 2769.
(15) Angel, L.; Stace, A. J. *J. Chem. Phys.* **1998**, *109*, 1713.
(16) Fehsenfeld, F. C.; Mosesman, M.; Ferguson, E. E. *J. Chem. Phys.* **1971**, *55*, 2120.
(17) Ishikawa, Y.; Binning, R. C.; Shramek, N. S. *Chem. Phys. Lett.* **1999**, *313*, 341.
(18) Frisch, M. J.; Trucks, G. W.; Schlegel, H. B.; Gill, P. M. W.; Johnson, B. G.; Robb, M. A.; Cheeseman, J. R.; Keith, T. A.; Petersson, G. A.; Montgomery, J. A.; Raghavachari, K.; Al-Laham, M. A.; Zakrzewski, V. G.; Ortiz, J. V.; Foresman, J. B.; Cioslowski, J.; Stefanov, B. B.; Nanayakkara, A.; Challacombe, M.; Peng, C. Y.; Ayala, P. Y.; Chen, W.; Wong, M. W.; Andres, J. L.; Replogle, E. S.; Gomperts, R.; Martin, R. L.; Fox, D. J.; Binkley, J. S.; Defrees, D. J.; Baker, J.; Stewart, J. P.; Head-Gordon, M.; Gonzalez, C.; Pople, J. A. *Gaussian 94*, Revision E.1; Gaussian, Inc.: Pittsburgh, PA, 1995.
(19) Curtiss, L. A.; Raghavachari, K.; Pople, J. A. *J. Chem. Phys.* **1993**, *98*, 1293.
(20) Curtiss, L. A.; Raghavachari, K.; Trucks, G. W.; Pople, J. A. *J. Chem. Phys.* **1991**, *94*, 7221.
(21) Nguyen, M.-T.; Hegarty, A. F. *J. Chem. Soc., Perkin Trans. 2* **1984**, 2043.
(22) Mó, O.; Yañez, M.; Elguero, J. *J. Chem. Phys.* **1992**, *97*, 6628.
(23) Kim, K. S.; Dupuis, M.; Lie, G. C.; Clementi, E. *Chem. Phys. Lett.* **1986**, *131*, 451.
(24) Cheng, B.-M.; Lee, J.-W.; Lee, Y.-P. *J. Phys. Chem.* **1991**, *95*, 2814.
(25) Benton, D. J.; Moore, P. *J. Chem. Soc. A* **1970**, 3179.
(26) McGrath, M. P.; Rowland, F. S. *J. Phys. Chem.* **1994**, *98*, 1061.
(27) Cunningham, A. J.; Payzant, J. D.; Kebarle, P. *J. Am. Chem. Soc.* **1972**, *94*, 7627.
(28) Yeh, L. I.; Okumura, M.; Myers, J. D.; Price, J. M.; Lee, Y. T. *J. Chem. Phys.* **1989**, *91*, 7319.
(29) Termath, V.; Sauer, J. *Mol. Phys.* **1997**, *91*, 963.
(30) Valeev, E. F.; Schaefer, H. F. *J. Chem. Phys.* **1998**, *108*, 7197.